Role of the clathrin adaptor PICALM in normal hematopoiesis and polycythemia vera pathophysiology

Yuichi Ishikawa,[1,2,3] Manami Maeda,[1,2] Mithun Pasham,[4,5,6] Francois Aguet,[4] Silvia K. Tacheva-Grigorova,[4,5,6] Takeshi Masuda,[2] Hai Yi,[2,7] Sung-Uk Lee,[1,2] Jian Xu,[8] Julie Teruya-Feldstein,[9] Maria Ericsson,[4] Ann Mullally,[2] John Heuser,[10] Tom Kirchhausen,[4,5,6] and Takahiro Maeda[1,2]

[1]Division of Hematopoietic Stem Cell and Leukemia Research, Beckman Research Institute of the City of Hope, Duarte, CA, USA; [2]Division of Hematology, Department of Medicine, Brigham and Women's Hospital, Harvard Medical School, Boston, MA, USA; [3]Department of Hematology and Oncology, Nagoya University Graduate School of Medicine, Japan; [4]Department of Cell Biology, Harvard Medical School, Boston, MA, USA; [5]Department of Pediatrics Harvard Medical School, Boston, MA, USA; [6]Program in Cellular & Molecular Medicine, Boston Children's Hospital, MA, USA; [7]Department of Hematology, General Hospital of Chengdu Military Region, Chengdu, China; [8]Children's Research Institute, Department of Pediatrics, University of Texas Southwestern Medical Center, Dallas, TX, USA; [9]Department of Pathology, Sloan-Kettering Institute, Memorial Sloan-Kettering Cancer Center, New York, NY, USA; [10]Department of Cell Biology and Physiology, Washington University School of Medicine, St. Louis, MO, USA

ABSTRACT

Clathrin-dependent endocytosis is an essential cellular process shared by all cell types. Despite this, precisely how endocytosis is regulated in a cell-type-specific manner and how this key pathway functions physiologically or pathophysiologically remain largely unknown. *PICALM*, which encodes the clathrin adaptor protein PICALM, was originally identified as a component of the *CALM/AF10* leukemia oncogene. Here we show, by employing a series of conditional *Picalm* knockout mice, that PICALM critically regulates transferrin uptake in erythroid cells by functioning as a cell-type-specific regulator of transferrin receptor endocytosis. While transferrin receptor is essential for the development of all hematopoietic lineages, Picalm was dispensable for myeloid and B-lymphoid development. Furthermore, global *Picalm* inactivation in adult mice did not cause gross defects in mouse fitness, except for anemia and a coat color change. Freeze-etch electron microscopy of primary erythroblasts and live-cell imaging of murine embryonic fibroblasts revealed that Picalm function is required for efficient clathrin coat maturation. We showed that the PICALM PIP_2 binding domain is necessary for transferrin receptor endocytosis in erythroblasts and absolutely essential for erythroid development from mouse hematopoietic stem/progenitor cells in an erythroid culture system. We further showed that *Picalm* deletion entirely abrogated the disease phenotype in a *Jak2*^{V617F} knock-in murine model of polycythemia vera. Our findings provide new insights into the regulation of cell-type-specific transferrin receptor endocytosis *in vivo*. They also suggest a new strategy to block cellular uptake of transferrin-bound iron, with therapeutic potential for disorders characterized by inappropriate red blood cell production, such as polycythemia vera.

Introduction

Erythroblasts take up transferrin-bound iron through the transferrin receptor (TfR) via clathrin-mediated receptor endocytosis.[1-3] Hemoglobin synthesis by red blood cells requires a large amount of iron,[4] so TfR endocytosis must be efficiently regulated. However, the factors promoting efficient TfR endocytosis in erythroblasts remain unclear. Such knowledge is key to our understanding of the pathogenesis of hematologic disorders, such as iron overload, anemia of chronic disease and hematologic malignancies.

PICALM, encoded by the *phosphatidylinositol binding clathrin assembly* (*PICALM*) gene, is a clathrin adaptor protein containing multiple domains functioning in clathrin-coated vesicle formation.[5-7] The *PICALM* gene, also known as *CALM* (*clathrin assembly lymphoid myeloid leukemia*), was originally identified as a component of the *CALM/AF10* leukemia oncogene.[8] Genome-wide association studies have recently demonstrated that single nucleotide polymorphisms in *PICALM* are strongly associated with the pathogenesis of Alzheimer disease.[9] Despite extensive efforts to understand its function, a precise role for PICALM in clathrin-mediated endocytosis remains largely unknown.

To determine the role of Picalm function in adult hematopoiesis precisely, we have generated a conditional knockout mouse strain in which *Picalm* can be deleted in a time- and tissue-specific manner. Here we show that PICALM is critical for clathrin-mediated TfR endocytosis in erythroblasts; however, it was dispensable for myeloid and B-lymphoid development. We further show that *Picalm* deletion abrogated the disease phenotype in a *Jak2*^{V617F} knock-in murine model of polycythemia vera (PV).

Methods

The gene-targeting strategy for *Picalm* mutant strains is illustrated in *Online Supplementary Figure S1B*. Standard methodology was used to

 doi:10.3324/haematol.2014.119537
The online version of this article has a Supplementary Appendix.
Manuscript received on October 22, 2014. Manuscript accepted on December 18, 2014.
Correspondence: tmaeda@partners.org

obtain targeted mutation of *Picalm* in non-agouti black Bruce4 C57BL/6-Thy1.1 mouse embryonic stem cells.

Results

Picalm-deficient embryos exhibit anemia and late-stage embryonic lethality

Primary mouse hematopoietic cells from bone marrow and spleen were sorted by fluorescence activated cell sorting (FACS) and analyzed by western blotting. Picalm protein was predominantly expressed in erythroblasts (Figure 1A). Picalm expression was also abundant in other non-hematopoietic tissues, while Ap180, a Picalm homolog, was expressed predominantly in brain tissue (*Online Supplementary Figure S1A*). Unique isoforms of Picalm protein were evident in muscle and brain (*Online Supplementary Figure S1A*). As observed in mouse cells, PICALM protein was induced in human erythroid cells when $CD34^+$ hematopoietic stem/progenitors were induced into an erythroid lineage (*Online Supplementary Figure S1B*).[10]

We next undertook gene targeting to generate mice carrying either one copy of the knockout allele ($Picalm^{+/-}$) or a floxed allele ($Picalm^{F/+}$) (*Online Supplementary Figure S1C*). In $Picalm^{-/-}$ embryos, no Picalm protein was detected by western blot using antibodies raised against either the Picalm N- or C-terminal, confirming successful *Picalm* deletion (*Online Supplementary Figure S1D* and *data not shown*). $Picalm^{-/-}$ mice were not viable, dying at late embryonic stages (*Online Supplementary Figure S1E*), although the cause of this *in utero* death is unclear. $Picalm^{-/-}$ embryos were smaller and paler than wild-type (WT) and heterozygous littermates (*Online Supplementary Figure S1F*). At late embryonic stages, immunohistochemical analysis indicated high cytoplasmic expression of Picalm protein which was distributed in a punctate pattern within cells of WT fetal liver, where definitive hematopoiesis occurs (Figure 1B).

Stages of erythroid development in fetal liver can be characterized by FACS based on expression of TER119 and TfR (CD71) (Figure 1C).[11] In $Picalm^{-/-}$ fetal liver cells, the proportion of R4, a more mature population consisting mainly of poly/ortho-chromatophilic erythroblasts, was significantly decreased, while that of R2, an immature population, increased, suggesting that Picalm is required for terminal erythroid differentiation (Figure 1D). In agreement, at 14.5 d.p.c. total fetal liver cell counts were significantly lower in $Picalm^{-/-}$ embryos (Figure 1E). Of note, enucleation, revealed by Hoechst stain,[12] took place normally in *Picalm*-deficient erythroblasts (*Online Supplementary Figure S1G*). *Picalm* heterozygotes ($Picalm^{+/-}$) were grossly normal and viable, exhibiting a very mild microcytic anemia (*Online Supplementary Figure S1H*).

Iron-deficient anemia in hematopoietic-specific Picalm conditional knockout mice

We generated hematopoietic-specific *Picalm* knockout mice ($Picalm^{F/F}$ $Mx1Cre^+$) to assess *Picalm* function in adult hematopoiesis. In this model, Cre recombinase is induced effectively in hematopoietic stem cells by polyinosinic-polycytidylic acid (pIpC) treatment.[13] Polymerase chain reaction genotyping and western blotting confirmed efficient *Picalm* deletion in hematopoietic cells (*Online Supplementary Figure S2A* and *data not shown*). Peripheral blood counts were analyzed for up to 1 year after pIpC injection. *Picalm*-deficient mice were anemic, as evidenced by significant reductions in red blood cell numbers, hemoglobin and hematocrit (Figure 1F). The anemia was microcytic and hypochromic, as the mean corpuscular volume, average red blood cell volume, and mean corpuscular hemoglobin were markedly low (Figure 1G). Benzidine staining of peripheral blood also suggested reduced intracellular hemoglobin levels and variability in red blood cell size (Figure 1H). Reticulocyte counts were elevated (Figure 1I) and red cell distribution width, an indicator of variability in red blood cell size and a value typically high in iron-deficient anemia, was significantly high in peripheral blood of *Picalm* knockout mice (Figure 1J). Variations in cell size and shape were also evidenced by Wright-Giemsa staining of peripheral blood smears (*Online Supplementary Figure S2B*). *Picalm*-deficient reticulocytes had a low hemoglobin content and a maturation defect, as indicated by reduced reticulocyte hemoglobin content and an increase of percentage immature reticulocyte fraction (%IRF) (*Online Supplementary Figure S2C*). Despite the iron-deficiency seen in red cells, serum iron levels were elevated in $Picalm^{F/F}$ $Mx1Cre^+$ mice (Figure 1K), suggesting that iron uptake pathways and/or the hemoglobinization process are impaired in *Picalm*-deficient erythroid cells. In contrast to the situation in clinically prevalent iron-deficiency anemia, total iron binding capacity was unchanged and transferrin saturation was slightly elevated (Figure 1L). $Picalm^{F/F}$ $Mx1Cre^+$ mice did not have a short life span, despite anemia, and tolerated phenylhydrazine-induced hemolytic stress (*Online Supplementary Figure S2D*). As expected, *Picalm*-deficient megakaryocyte/erythroid progenitors gave rise to fewer colonies in colony-forming assays, and individual colonies were smaller than those of controls (*Online Supplementary Figure S2E* and *data not shown*). Although the difference was not statistically significant, platelet counts were slightly high in $Picalm^{F/F}$ $Mx1Cre^+$ mice (Figure 1M).

Picalm is dispensable for myeloid and B-lymphoid development

To determine whether Picalm is required for the development of all hematopoietic cells, as is TfR,[14] we examined myeloid and lymphoid cell counts over time in peripheral blood upon *Picalm* deletion. Total white blood cell counts were comparable to those in controls (Figure 2A), while T-cell counts were slightly low in $Picalm^{F/F}$ $Mx1Cre^+$ mice (Figure 2A). T-cell development in the thymus was grossly normal (Figure 2B) and development of non-erythroid cells in the bone marrow was unaffected in $Picalm^{F/F}$ $Mx1Cre^+$ mice, while the proportion of R4 was significantly decreased (Figure 2C). Furthermore, stem/progenitor populations in the bone marrow were unaffected in $Picalm^{F/F}$ $Mx1Cre^+$ mice (Figure 2D). In agreement with the findings in $Picalm^{F/F}$ $Mx1Cre^+$ mice, B-cell-specific *Picalm* knockout mice ($Picalm^{F/F}$ $mb1Cre^+$) exhibited normal B-cell development in the steady state (*Online Supplementary Figure S3A,B*). Furthermore, germinal center B cells developed normally upon immunization with T-cell-dependent antigen (*Online Supplementary Figure S3C*), indicating that Picalm is dispensable for B-cell development.

To determine whether observed phenotypes in $Picalm^{F/F}$ $Mx1Cre^+$ mice are caused by cell-autonomous mechanisms, we performed a bone marrow reconstitution assay

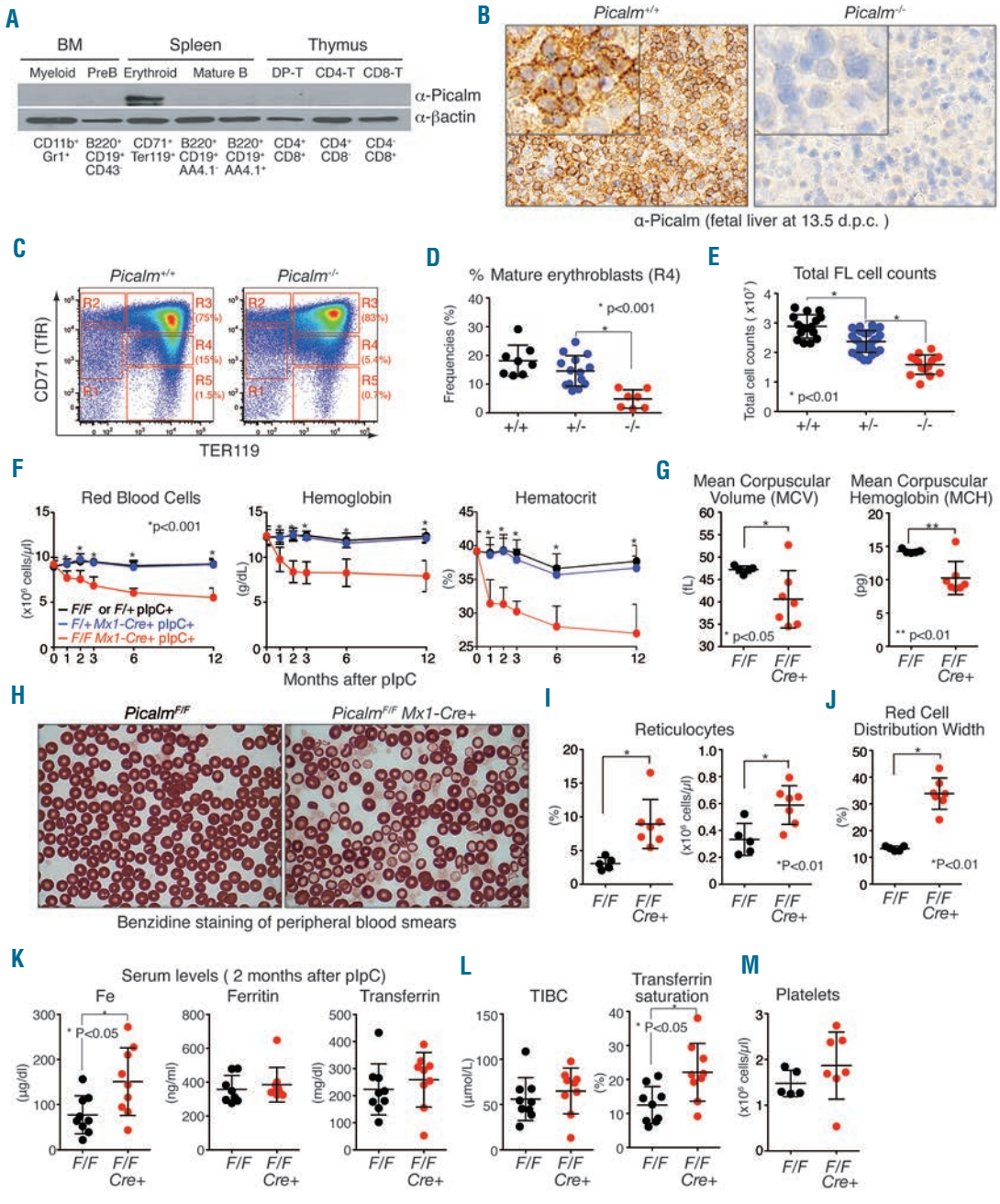

Figure 1. *Picalm* knockout mice develop microcytic and hypochromic anemia. (A) Picalm is predominantly expressed in erythroid cells. Mouse hematopoietic cells from bone marrow (BM), spleen or thymus were FACS-sorted using lineage-specific surface markers. Picalm protein levels were analyzed by western blot using anti-Picalm antibody. (B) Immunohistochemical analysis for Picalm was performed on formalin-fixed, paraffin-embedded fetal liver (FL) sections of 13.5 d.p.c. embryos. Brown stains in WT FL represent Picalm protein. Complete absence of Picalm protein in *Picalm*$^{-/-}$ FL confirmed successful *Picalm* deletion *in vivo*. Insets: high magnification images. (C) Erythroid development in FL was analyzed by FACS based on surface expression levels of TER119 and CD71 (TfR). Each gate (R1 to R5) was determined as described.[11] Representative FACS profiles of *Picalm*$^{+/+}$ or *Picalm*$^{-/-}$ FL cells from 14.5 d.p.c. embryos are shown. (D) Dot graph shows proportions of R4 erythroblasts (TER119^{+}CD71^{dim+}), which consist mainly of ortho-chromatophilic erythroblasts and reticulocytes. Horizontal black bars: average value; error bars: standard deviation. (E) Absolute counts of 14.5 d.p.c. FL cells, which consist mainly of erythroid lineage cells. Horizontal black bars: average value; error bars: standard deviation. (F) Time-course analysis of peripheral blood (PB) upon pIpC injection. Three pIpC doses (250 μg/injection) were administered intraperitoneally as described elsewhere[51]. PB counts were examined at indicated time points after injections. *Picalm*$^{F/F}$ *Mx1Cre*$^{+}$ mice, but not *Picalm*$^{F/+}$ *Mx1Cre*$^{+}$ or control mice (*Picalm*$^{F/+}$ or *Picalm*$^{F/F}$), exhibited a marked reduction in red blood cell counts, hemoglobin and hematocrit. Each plot represents average values of 10-18 mice; error bars: standard deviation. (G) Dot graphs represent average red blood cell size and average amount of hemoglobin per red blood cell 3 months after pIpC injections. Error bars: standard deviation. (H) PB smears stained with benzidine, which stains hemoglobin. Benzidine-negative/dim red blood cells, which contain low concentrations of intracellular hemoglobin, are evident in PB smears of *Picalm*$^{F/F}$ *Mx1Cre*$^{+}$ mice. Sizes and shape of *Picalm*-deficient red blood cells are more variable than those of control samples. (I) Proportions (left) and absolute counts (right) of reticulocytes 3 months after pIpC injections. Horizontal black bars: average value; error bars: standard deviation. (J) Red cell distribution width (RDW), a measure of deviation in red blood cell volume in PB, was markedly increased in *Picalm*$^{F/F}$ *Mx1Cre*$^{+}$ mice. RDW was measured 3 months after pIpC injections. Horizontal black bars: average value; error bars: standard deviation. (K) Levels of iron (Fe), ferritin and transferrin in serum were measured 2 months after pIpC injections. Serum Fe levels in *Picalm*$^{F/F}$ *Mx1Cre*$^{+}$ mice were higher than those of controls, while ferritin and transferrin levels were comparable to those in controls. Horizontal black bars: average value; error bars: standard deviation. (L) Total iron binding capacity (TIBC) and transferrin saturation (%). Horizontal black bars: average value; error bars: standard deviation. (M) Platelets counts 3 months after pIpC injections. Horizontal black bars: average value; error bars: standard deviation.

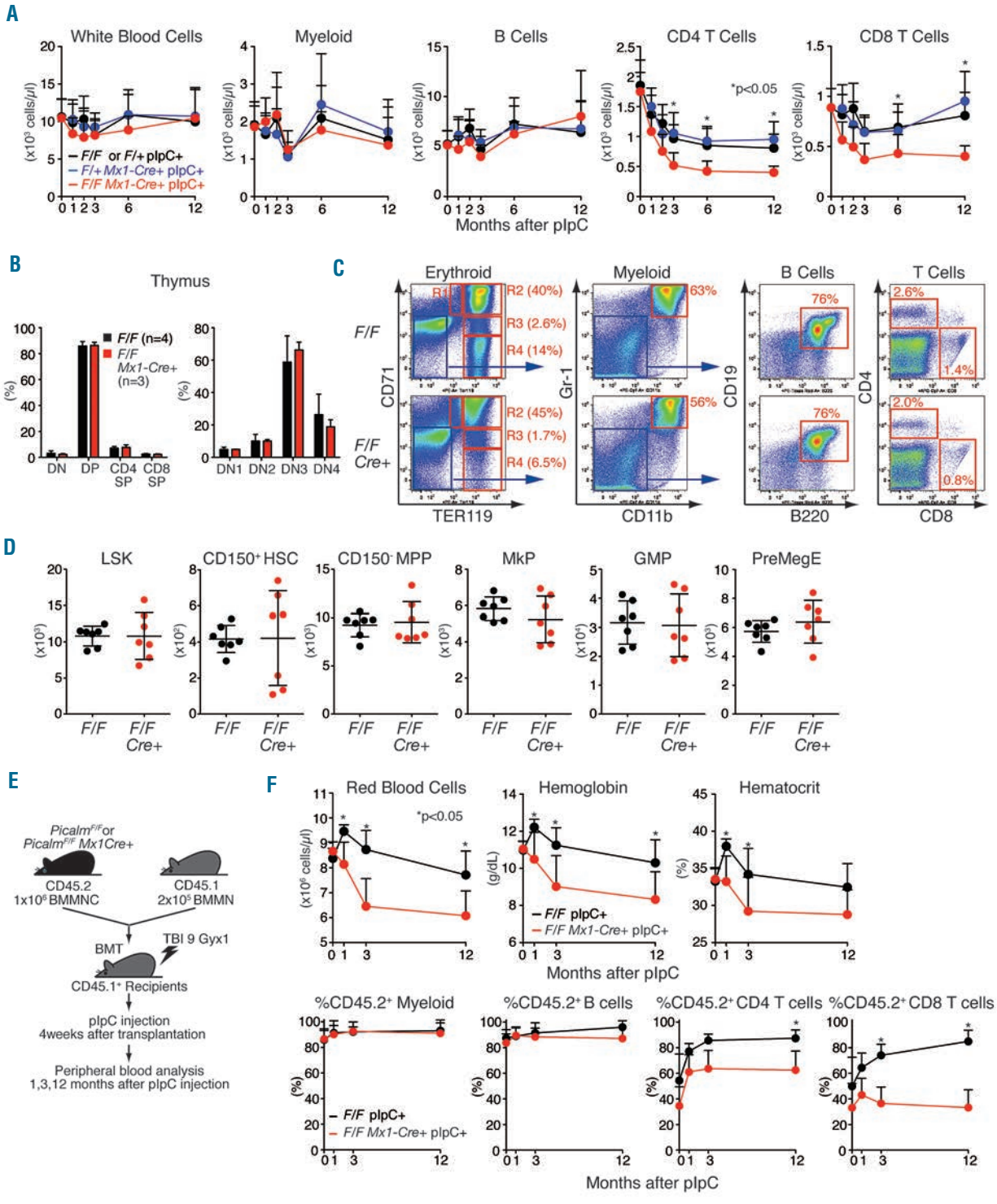

Figure 2. Picalm is dispensable for myeloid and B-lymphoid development. (A) Time-course analysis of non-erythroid cells in peripheral blood upon pIpC injection. White blood cell counts were examined at indicated time points after injections. Proportions of myeloid and lymphoid cells were determined by FACS. Each plot represents average value of 10-18 mice; error bars: standard deviation. (B) Graph shows frequencies of CD4/8 double-negative (DN), CD4/8 double-positive (DP), CD4 single-positive (CD4SP) and CD8 single-positive (CD8SP) T cells 2 months after pIpC injections (left). Frequencies of DN fractions (DN1: CD44$^+$CD25$^-$, DN2: CD44$^+$CD25$^+$, DN3: CD44$^-$CD25$^+$ and DN4: CD44$^-$CD25$^-$) are also shown (right). (C) Representative FACS profiles of bone marrow cells from control (*Picalm*$^{F/F}$) and *Picalm* knockout mice (*Picalm*$^{F/F}$ *Mx1Cre*$^+$) 2 months after pIpC injections. (D) Dot graphs of absolute counts (per leg) of hematopoietic stem/progenitors in bone marrow 2 months after pIpC injections. Stem/progenitors were identified by FACS as described elsewhere[62]. LSK (lineage-Sca1$^+$c-Kit$^+$); HSC (hematopoietic stem cells); MPP (multi-potential progenitors); MkP (megakaryocyte progenitors); GMP: granulocyte macrophage progenitors; PreMegE (pre-megakaryocyte–erythrocyte progenitors). Horizontal black bars: average value; error bars: standard deviation. (E) Schematic representation of a bone marrow transplant experiment. One million bone marrow mononuclear cells (BMMNC) from either control (*Picalm*$^{F/F}$) or knockout (*Picalm*$^{F/F}$ *Mx1Cre*$^+$) mice were transferred to a lethally-irradiated (9 Gy, single dose) recipient mouse along with CD45.1$^+$ 2 x 10^5 BMMNC (competitors). Recipients were injected with pIpC 1 month after transplantation (250 μg x 3). (F) Peripheral blood counts were analyzed by a hematology analyzer and FACS 1, 3 and 12 months after pIpC injections. Each dot represents the average value of 12 samples in each group; error bars: standard deviation.

(Figure 2E). Recipients of bone marrow reconstituted with *Picalm*$^{F/F}$ *Mx1Cre*$^{+}$ cells developed anemia after pIpC administration (Figure 2F), indicating that the anemia seen in *Picalm*$^{F/F}$ *Mx1Cre*$^{+}$ mice was caused by cell-intrinsic mechanisms. While *Picalm*-deficient myeloid and B-lymphoid cells comprised 80-100% of donor-derived cells, *Picalm*-deficient T cells exhibited a competitive disadvantage with respect to competitor-derived cells, suggesting that the T-lymphopenia observed in *Picalm*$^{F/F}$*Mx1Cre*$^{+}$ mice also occurred cell-autonomously (Figure 2F).

Transferrin receptor endocytosis is significantly attenuated in Picalm-deficient erythroblasts

The extent of erythroid differentiation in the spleen can be characterized by FACS based on cell size (forward scatter: FSC) and levels of expression of TER119, CD71 and CD44.[15,16] A relative increase in the number of immature erythroblasts (R2) and a concomitant decrease in the number of mature erythroblasts (R4) were evident in spleens of *Picalm*$^{F/F}$ *Mx1Cre*$^{+}$ mice (Figure 3A,B). *Picalm*$^{F/F}$ *Mx1Cre*$^{+}$ mice also showed a markedly impaired transition from stage III (consisting mainly of poly-chromatophilic erythroblasts) to stage IV (consisting of ortho-chromatophilic erythroblasts and reticulocytes) (Figure 3B). Stage II and III cells, which were predominantly benzidine-positive in WT erythroblasts, were mostly benzidine-negative in *Picalm*$^{F/F}$ *Mx1Cre*$^{+}$ mice (Figure 3C), suggesting that iron-deficiency caused by *Picalm* depletion precludes differentiation from poly- to ortho-chromatophilic erythroblasts. We also found that reduced numbers of mature erythroblasts in *Picalm* knockout mice were due, at least in part, to increased apoptosis of erythroblasts (Figure 3D). Serum erythropoietin levels were significantly high (Figure 3E) and the spleen was enlarged in *Picalm*$^{F/F}$ *Mx1Cre*$^{+}$ mice (Figure 3F).

To assess the efficiency of transferrin/TfR endocytosis in a quantitative manner, we established a FACS-based TfR endocytosis assay (Figure 4A). Amounts of surface-bound transferrin markedly increased in *Picalm*-deficient erythroblasts, particularly those of basophilic and poly-chromatophilic erythroblasts (Figure 4B). Mean fluorescence intensity of internalized transferrin was significantly higher relative to that of surface-bound transferrin in WT erythroblasts; however, it was not in *Picalm*-deficient cells (Figure 4B). Transferrin/TfR endocytosis was nearly 25% as efficient in *Picalm*-deficient compared to WT erythrob-

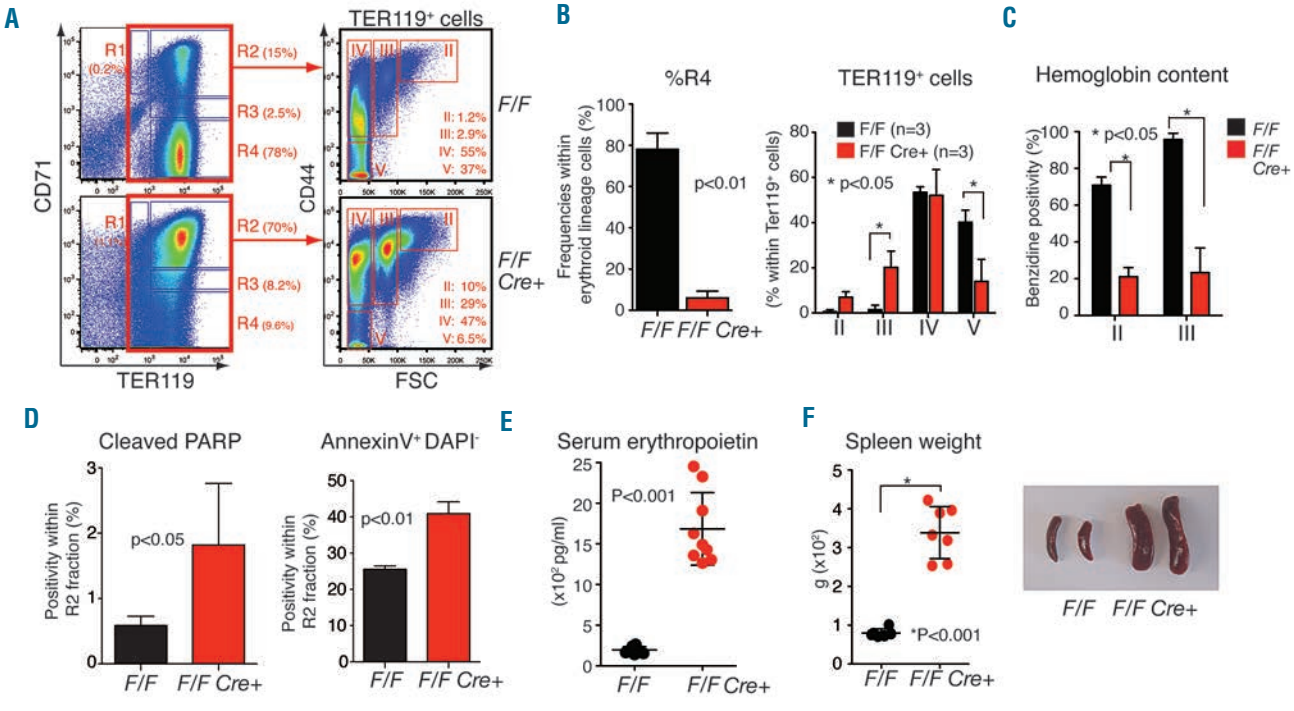

Figure 3. Inefficient erythroid development in *Picalm*$^{F/F}$ *Mx1Cre*$^{+}$ mice. (A) Representative FACS profiles of splenic erythroblasts from control (*Picalm*$^{F/F}$) and *Picalm* knockout mice (*Picalm*$^{F/F}$ *Mx1Cre*$^{+}$) 2 months after pIpC injections. Immature erythroblasts (R2) did not efficiently give rise to mature erythrocytes (R4). (B) Bar graphs show proportions of R4 erythroblasts in the spleen 1 month after pIpC injections (left). Proportions of CD44/FSC-based sub-fractions[16] are also shown (right). Histograms: average value of three samples per genotype; error bars: standard deviation. (C) Benzidine staining of splenic erythroblasts. FACS-sorted erythroblasts were cyto-spun onto glass slides and stained with benzidine, an indicator of intracellular hemoglobin levels. Graph shows frequencies of benzidine-positive cells in stage II and III cells.[16] Almost all cells at stage III were benzidine-positive in control cells, while only 20% of *Picalm*-deficient erythroblasts stained positive. Histograms: average value of three samples per genotype; error bars: standard deviation. (D) Apoptosis of R2 erythroblasts was measured by FACS by appearance of cleaved PARP (left) and annexin V-staining (right) 2 months after pIpC injections. Histograms: average value of four samples per genotype; error bars: standard deviation. (E) Dot graph shows serum erythropoietin levels 2 months after pIpC injections. In response to hypoxia in the periphery, erythropoietin levels in *Picalm* knockout mice were 20-fold higher than those seen in controls. Horizontal black bars: average value; error bars: standard deviation. (F) Dot graphs represent average spleen weight 2 months after pIpC injections (left). Horizontal black bars: average value; error bars: standard deviation. Representative picture of spleens (right).

lasts (Figure 4C). Total TfR protein levels in *Picalm*-deficient erythroblasts were comparable to those in control cells (Figure 4D), suggesting that TfR endocytosis, but not its expression, is regulated by Picalm. Of note, regardless of high TfR expression, Picalm was barely detected in bone marrow macrophages (Figure 4D). Importantly, amounts of surface-bound and internalized Alexa647-transferrin were unchanged in B-lymphoid and myeloid cells regardless of the genotype (*Online Supplementary Figure S3D*).

Picalm is necessary for clathrin-coat maturation

To further understand the role of Picalm in clathrin-coated vesicle formation in erythroblasts, we performed freeze-etch electron microscopy.[17] The representative images indicated a decrease in the number of fully-formed clathrin coated pits in *Picalm*-deficient erythroblasts when compared to images from WT cells (Figure 5A and *Online Supplementary Figure S4A*). Clathrin-mediated TfR endocytosis is a dynamic process consisting of multiple steps (Figure 5B).[18] We established immortalized mouse embryonic fibroblasts (MEF) in which *Picalm* can be deleted in an inducible manner (*Picalm*$^{F/F}$ *ERT2-Cre*$^{+}$ MEF) (Figure 5C). We then stably transduced these MEF with retrovirus encoding an EGFP-tagged adaptin σ2 (σ2-EGFP) that efficiently co-assembled with the endocytic clathrin adaptor AP2 complex to image dynamic processes of clathrin-coated pit formation.[19,20] As Picalm was almost completely depleted by 48 h after tamoxifen treatment (Figure 5C), we carried out our experiments using MEF treated with vehicle or tamoxifen for 72 h.

We first performed electron microscopy in MEF upon induction of *Picalm* deletion. We observed a substantial increase in the shallow pit fraction and a decrease in the fraction of mature vesicles in *Picalm*$^{F/F}$ *ERT2-Cre*$^{+}$ MEF upon tamoxifen treatment (Figure 5D). We then used live cell spinning-disk confocal fluorescence microscopy to characterize the consequences of depleting *Picalm* in the formation dynamics of AP2-containing endocytic clathrin-coated structures. Assembly of the clathrin/AP2 coats at

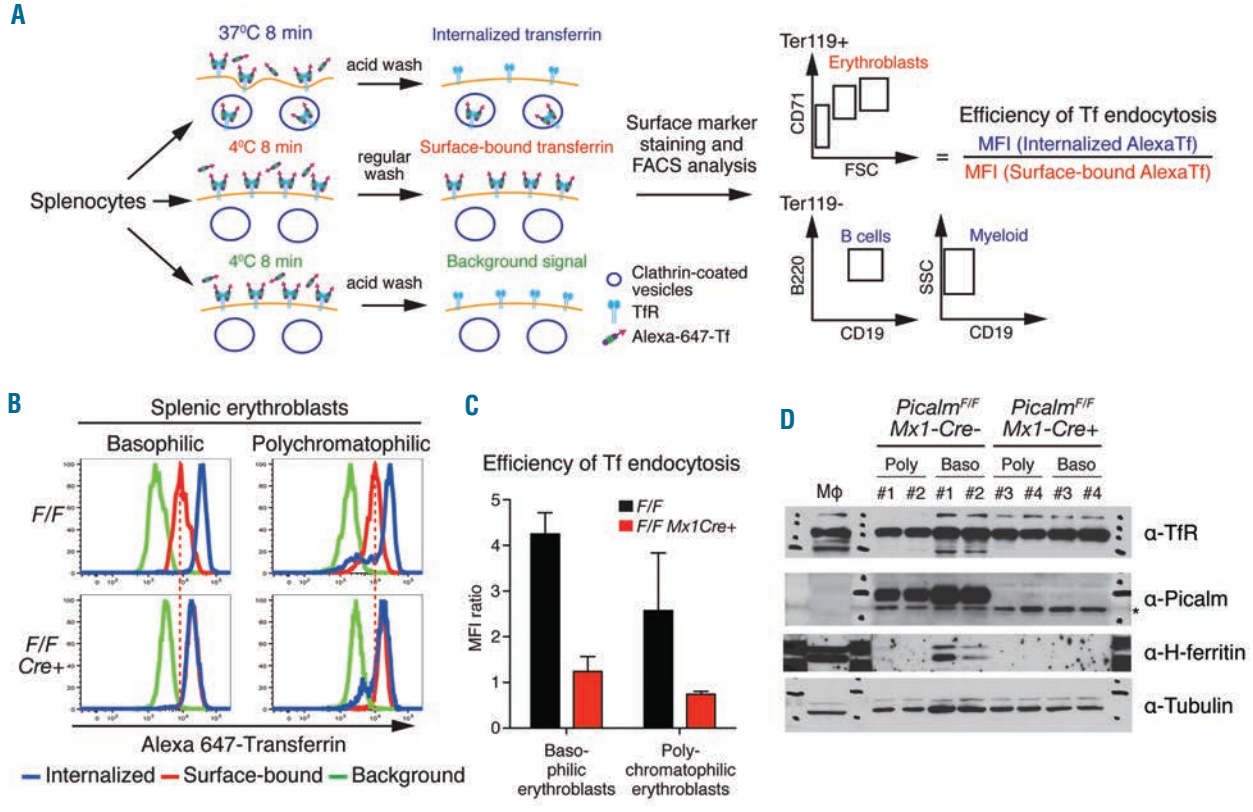

Figure 4. TfR endocytosis is impaired in *Picalm*-deficient erythroblasts. (A) FACS-based transferrin/TfR endocytosis assay. To measure the amount of internalized transferrin, splenocytes were incubated at 37°C for 8 min with Alexa-647 transferrin, chilled to 4°C (to stop endocytosis) and washed with low-pH buffer to remove transferrin bound to the cell surface. For surface-bound transferrin, cells were incubated at 4°C with Alexa-647 transferrin and then washed with neutral pH buffer. Samples were then incubated with fluorescently-tagged antibodies specific for erythroid and lymphoid cells and subjected to FACS analysis. As a background control, splenocytes were incubated with at 4°C with Alexa-647 transferrin for 8 min, washed with acid buffer and analyzed by FACS. Efficiency of transferrin (Tf) endocytosis was calculated by dividing mean fluorescence intensity (MFI) of internalized transferrin by that of surface-bound transferrin. (B) Representative FACS profiles of transferrin/TfR endocytosis assay in erythroblasts. MFI of internalized- (blue lines) and surface bound- (red lines) transferrin was measured by FACS at different stages of erythroid differentiation. Background signals are also presented for each population (green lines). Red-dashed lines indicate levels of surface-bound Alexa-transferrin in control erythroblasts. (C) Bar graphs show efficiencies of transferrin endocytosis in basophilic and polychromatophilic erythroblasts. Experiments were repeated three times, and representative results are presented. Histograms: average value of two samples per genotype; error bars: standard deviation. (D) Western blot for TfR in FACS-sorted erythroblasts. Samples from two mice per genotype (control: #1 and #2, *Picalm* knockout: #3 and #4) were analyzed. TfR protein levels in *Picalm*-deficient erythroblasts were comparable to those of controls. Western blot for H-ferritin, indicative of intracellular iron storage; Picalm and Tubulin are also shown. Mφ: protein lysates of bone marrow macrophages. Asterisk: non-specific signal.

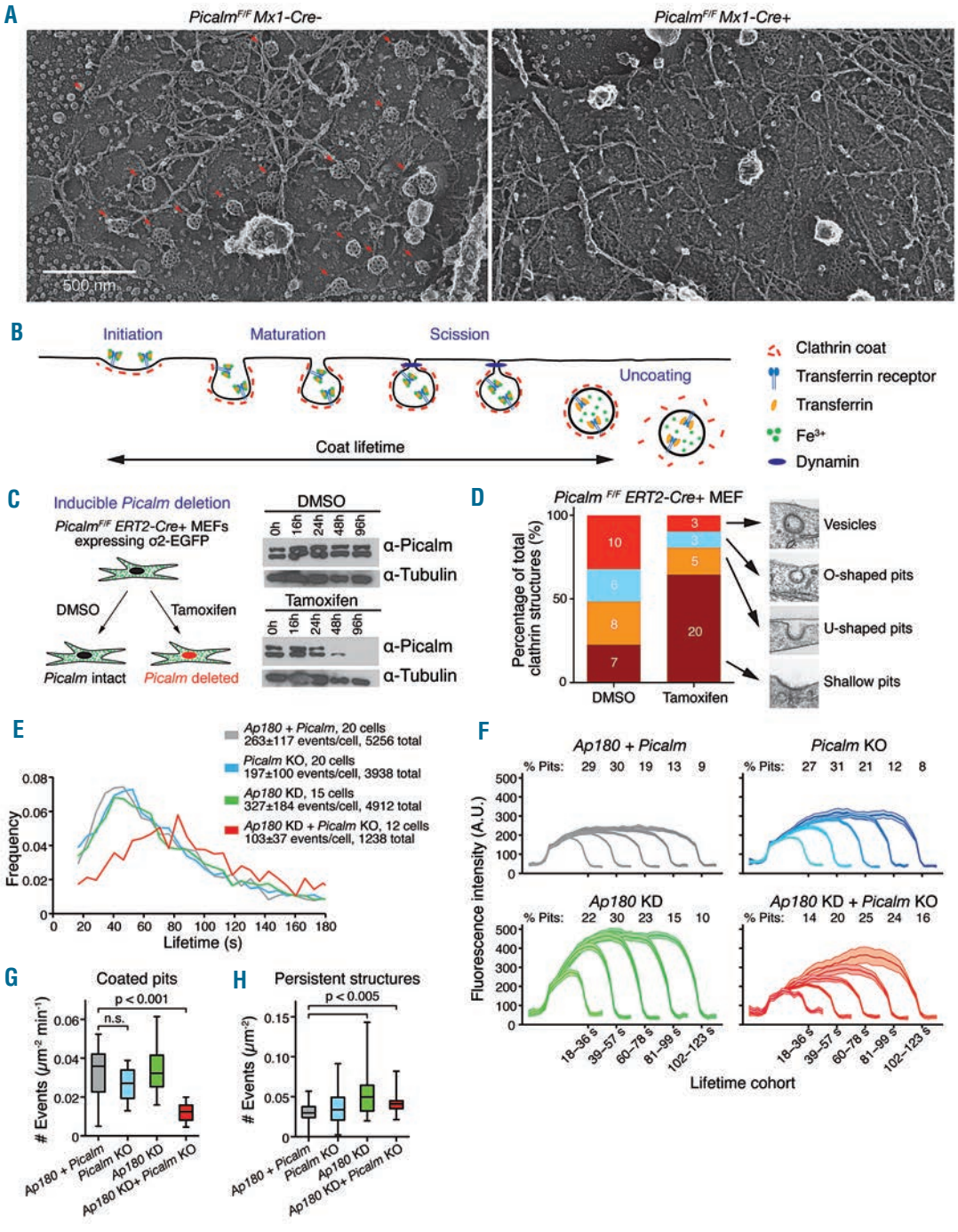

Figure 5. Formation of clathrin-coated vesicles in *Picalm*-deficient cells. (A) Representative pictures of freeze-etch electron microscopy in primary splenic erythroblasts. Formation of mature vesicles was barely observed in *Picalm*-deficient erythroblasts. Arrows indicate clathrin-coated vesicles. (B) Formation of endocytic clathrin-coated structures on the plasma membrane. The process of clathrin-dependent endocytosis is dynamic and has multiple steps, including initiation, maturation, scission and uncoating. (C) Generation of mouse embryonic fibroblasts (MEF) in which *Picalm* is inducibly deleted by tamoxifen treatment (*Picalm*$^{F/F}$ *ERT2-Cre*$^{+}$ MEF). MEF were established from a 13.5 d.p.c *Picalm*$^{F/F}$ *ERT2-Cre*$^{+}$ embryo, immortalized with large T antigen and retrovirally transduced with EGFP-tagged AP2-bound adaptin σ2 (σ2-EGFP).[19,20] Western blot for Picalm confirmed inducible depletion of Picalm protein in tamoxifen-treated but not control DMSO-treated MEF (right). Two splice forms of Picalm (Picalm-long and -short) were evident in MEF, and both were absent after tamoxifen treatment. (D) Relative frequency of each clathrin structure was measured 72 h after tamoxifen (or DMSO) treatment of *Picalm*$^{F/F}$ *ERT2-Cre* MEF. The proportion of mature vesicles was significantly reduced in tamoxifen-treated (*Picalm*-deleted) MEF. (E) Summary of the various cell types used to acquire live-cell imaging data using spinning-disk confocal microscopy of *Picalm*$^{F/F}$ *ERT2-Cre*$^{+}$ MEF cells stably expressing AP2 (σ2-EGFP). *Picalm* KO denotes *Picalm* deletion by tamoxifen addition; *Ap180* KD denotes *Ap180* knockdown by shRNA. The general statistics indicate the number of cells analyzed per condition as well as the average ± SD of coated pits (events) per cell and the total number of events detected using the tracking algorithm described by Aguet *et al.*[21] Coated pits are structures that gained fluorescence intensity relative to the first detected time point. The plot shows the lifetime distributions for coated pits. (F) Plots corresponding to the average fluorescence intensities from the corresponding number of cells, calculated from productive coated pit trajectories binned by lifetime represented as mean intensity (solid lines) and standard error (shaded areas). The top of each graph indicates the average percentage of coated pits within each cohort. (G) The panel corresponds to the area density of coated pits that formed per min during the 5 min duration of the time-series. (H) The panel shows the density of persistent structures, defined as structures present for the full duration of the time-series. Box plots show median, 25th, and 75th percentiles, and outermost data points. Statistical significance was determined using the permutation test for medians.

the surface of the MEF attached to the glass coverslip was followed using an automated unbiased tracking approach.[21] Whereas loss of *Picalm* or *Ap180* alone had no noticeable effects on coat dynamics, simultaneous deletion of *Picalm* (knockout) and short hairpin RNA-mediated knock-down of *Ap180* (*Online Supplementary Figure S4B,C*) led to a significant increase in the lifetime of the coated pits/vesicles (Figure 5E,F) together with a substantial decrease in the number of coated pits (Figure 5G); the number of long-lasting structures (plaques) was only slightly affected (Figure 5H).

The Picalm PIP_2 binding domain is essential for transferrin receptor endocytosis

Picalm binds to r-soluble NSF attachment protein receptors (r-SNARE) and to the plasma membrane phosphatidylinositol 4,5-bisphosphate (PIP_2) through its N-terminal ANTH (AP180 N-terminal homology) domain and interacts with clathrin as well as other accessory proteins (Figure 6A).[5-7,22] Of note, Picalm normally exists as two splice isoforms that differ by inclusion or exclusion of exon 13, which encodes 51 amino acids exhibiting a DPF and an NPF motif (Figure 6A).

To determine amino acid residues/domains required for Picalm function in erythroblasts, we performed add-on rescue experiments using a series of Picalm mutants (Figure 6A and *Online Supplementary Figure S4D*). To do so, we established K562 erythro-leukemia cells stably expressing short hairpin RNA targeting *PICALM* and then "added-back" each PICALM mutant via retroviral transduction, followed by FACS-based transferrin endocytosis assays. Among mutants tested, PIP_2-PICALM, which cannot bind PIP_2 due to replacement of three lysine residues (38KKK40) with glutamic acid (38EEE40) (*Online Supplementary Figure S4D*),[6] failed to rescue transferrin uptake in *PICALM*-knockdown K562 cells (Figure 6C,D), indicating that PIP_2 binding is necessary for PICALM-mediated TfR endocytosis. Expression levels of PIP_2-PICALM protein was comparable to that of WT-PICALM, confirmed by western blotting (*Online Supplementary Figure S4E*). Addback of Picalm mutants unable to interact with the r-SNARE VAMP 2, 3 and 8, fully rescued the uptake of transferrin, suggesting that traffic of these r-SNARE is not required for efficient transferrin uptake. Similar results were obtained with the add-back of Picalm mutants unable to interact with either clathrin or AP2. In this case, maintaining either one of these interactions was sufficient to sustain efficient transferrin uptake.

Picalm/PIP_2 interaction is necessary for erythroid differentiation

To determine the function of PICALM/PIP_2 interaction in erythroid development, we employed a culture system that recapitulated erythroid differentiation from progenitors *in vitro*.[11,23] WT- and *Picalm*-deficient bone marrow cells were depleted of mature lineage marker-positive cells (erythroid, myeloid and lymphoid cells) in order to enrich the hematopoietic progenitors, and progenitors were then cultured in the presence of erythropoietin, holo-transferrin and insulin for 3 days (*Online Supplementary Figure S5A*).[23] Progenitors from control mice ($Picalm^{F/F}$) differentiated into mature erythroblasts after 3 days of culture, as previously described (Figure 6E,F).[11,23] In contrast, *Picalm*-deficient progenitors barely developed into an erythroid lineage (Figure 6E,F), and most cells remaining on day 3 were $CD11b^+$ myeloid cells. Wright-Giemsa staining of cytospin preparations showed enrichment of erythrocytes and erythroblasts in WT cells, while *Picalm*-deficient cells mainly consisted of myeloid lineage cells (segmented neutrophils, banded neutrophils and myeloblasts) (*Online Supplementary Figure S5B*). Ferric ammonium citrate incorporates into cells through "TfR-independent" mechanisms.[24] Importantly, treatment with ferric ammonium citrate dose-dependently restored development of *Picalm*-deficient mature erythroblasts (Figure 6G), indicating that lack of TfR-mediated iron uptake is the primary cause of erythroid defects seen in *Picalm*-deficient cells *in vitro*.

We next examined whether exogenous expression of WT- or PIP_2-PICALM would rescue erythroid differentiation in *Picalm*-deficient progenitors. To do so, we harvested bone marrow progenitor cells from $Picalm^{F/F}$ $Mx1Cre^+$ mice 1 month after pIpC injection, retrovirally transduced them with either WT- or PIP_2-PICALM and then induced erythroid differentiation (Figure 6H). Since the retrovirus also encodes a green fluorescent protein, we assessed the extent of erythroid differentiation in the fraction positive for this protein. As expected, WT-PICALM completely rescued erythroid differentiation in *Picalm*-deficient cells, while PIP_2-PICALM-transduced cells barely differentiated into mature cells (Figure 6I,J). We also tested a PICALM mutant in which the ANTH domain was replaced with the PH domain of rat phosphlipase C delta 1 (PH-PICALM), a motif that harbors a lipid-binding domain specific to PIP_2.[25] PH-PICALM failed to rescue erythroid differentiation in *Picalm*-deficient cells, indicating that PICALM binding to PIP_2 is necessary but not sufficient for erythroid differentiation.

Picalm inactivation ameliorates the pathophysiology of polycythemia vera in mice

Although Picalm was abundant in non-hematopoietic tissues (*Online Supplementary Figure S1A*), global *Picalm* inactivation in adult mice ($Picalm^{F/F}$ $ERT2\text{-}Cre^+$) did not cause gross defects in mouse fitness, except for anemia and a coat color change (*Online Supplementary Figure S6*). Upon intraperitoneal injections of tamoxifen, *Picalm* inactivation was achieved in all tissues examined except the brain (*Online Supplementary Figure S6A*). $Picalm^{F/F}$ $ERT2\text{-}Cre^+$ mice exhibited a microcytic and hypochromic anemia and inefficient erythroid differentiation in the spleen, as did $Picalm^{F/F}$ $Mx1\text{-}Cre^+$ mice (*Online Supplementary Figure S6B,C*). Picalm deficiency did not affect postnatal development and the body weights of $Picalm^{F/F}$ $ERT2\text{-}Cre^+$ mice were comparable to those of control mice (*Online Supplementary Figure S6D* and *data not shown*). Coat-color graying was observed upon *Picalm* inactivation, suggesting that Picalm functions in melanin synthesis and/or melanosome transfer (*Online Supplementary Figure S6E*). Considering that *Picalm* deletion limits terminal erythroid differentiation through the induction of iron depletion in erythroblasts and that Picalm is likely dispensable in non-hematopoietic tissues in adult animals, we sought to explore the impact of *Picalm* deletion in a disease characterized by an excess production of mature red blood cells, namely polycythemia vera (PV).

In PV, erythroid precursor cells aberrantly expand as a result of enhanced signaling downstream of the erythropoietin receptor due to an activating mutation in JAK2 kinase ($JAK2^{V617F}$). We crossed *Picalm* conditional knockout mice with a conditional knock-in $Jak2^{V617F}$ mouse model of PV

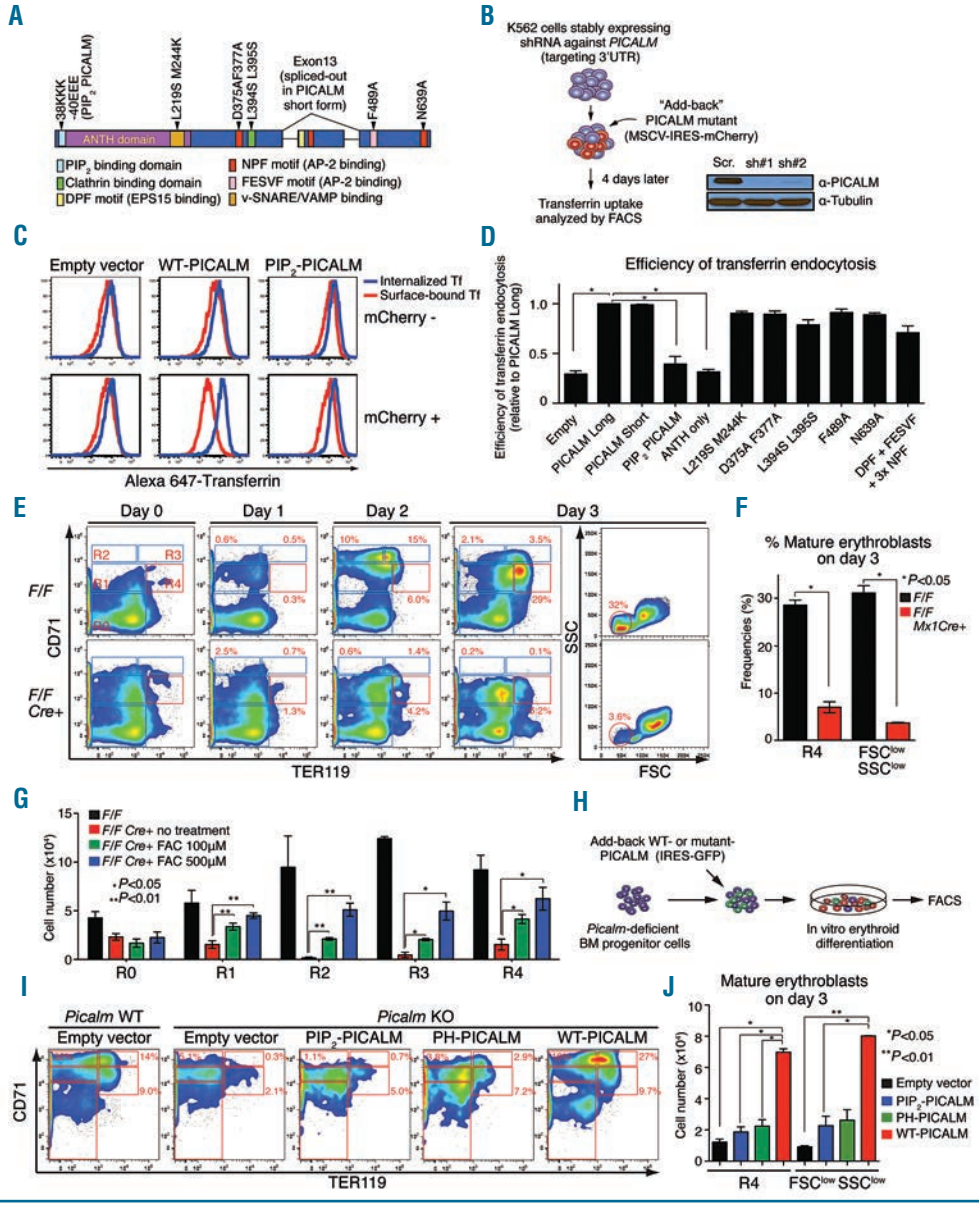

Figure 6. PICALM/PIP_2 interaction is critical for erythroid differentiation. (A) Structure of human PICALM protein and predicted domains/motifs. Exon 13 is spliced out in the PICALM short form. Every mutant defined at the top was tested for its capacity to rescue *PICALM* deficiency. Mutated residues in each mutant are described in *Online Supplementary Figure S4D*. (B) Experimental outline of "add-back" rescue experiments using *PICALM*-knockdown K562 leukemia cells (left). Lentivirus vectors encoding shRNA targeting the *PICALM* 3'UTR were generated, and knockdown efficiency in K562 leukemia cells was tested by western blot. K562 cells stably expressing *PICALM* shRNA#1 were used for the experiment (right). Each *PICALM* mutant was retrovirally "added-back" into *PICALM*-knockdown K562 cells and transferrin uptake analyzed 4 days after transduction. Retrovirus also encodes a mCherry fluorescent protein, allowing tracking of cells expressing mutant or WT *PICALM*. (C) FACS-based transferrin/TfR endocytosis assays were performed as described. Representative FACS profiles of empty vector-, WT-PICALM (long form)- and PIP_2-PICALM- infected cells are shown. (D) Efficiency of transferrin endocytosis in mCherry-positive cells was calculated as described in Figure 4A. Histograms show the relative efficiency of transferrin endocytosis upon "add-back" of empty vector or *PICALM* mutants. Transferrin endocytosis was significantly reduced in empty- or PIP_2-PICALM-transduced cells compared to that of WT-PICALM-transduced cells. In contrast, other PICALM mutants enhanced TfR endocytosis in *PICALM*-knockdown K562 cells up to levels seen with WT-PICALM. Histograms: average value of two to four samples per condition; error bars: standard deviation. (E) Erythroid development in culture was examined daily for 3 days after induction of erythroid differentiation. Representative FACS profiles of control- and *Picalm*-deficient cells are shown. The extent of erythroid differentiation was assessed by FACS based on surface marker expression levels (TER119 and CD71) and cell size [forward scatter (FSC) and side scatter (SSC)]. R4 cells ($TER119^+CD71dim^+$), which consist mainly of ortho-chromatophilic erythroblasts and reticulocytes, are depicted with red rectangles. Fully-differentiated erythroid cells are smaller than immature erythroblasts and fall into the FSC^{low} SSC^{low} fraction. (F) Bar graphs show frequencies of mature erythroblasts after 3 days of culture. *Picalm*-deficient stem/progenitors gave rise to markedly fewer mature erythroblasts compared to controls. Experiments were repeated at least four times, and representative results are presented. Histograms: average value of two samples per genotype; error bars: standard deviation. (G) Iron supplement treatment (ferric ammonium citrate: FAC) significantly enhanced erythroid development of *Picalm*-deficient progenitors in a dose-dependent manner. Bar graphs show cell counts of each fraction (R0-R4) on day 2 in the presence or absence of FAC in the culture medium. Experiments were repeated three times, and representative results are presented. (H) Functional rescue experiments. Bone marrow stem/progenitor cells were obtained from $Picalm^{F/F}Mx1Cre^+$ mice 2 months after plpC injections and transduced with retrovirus vectors encoding WT- or PIP_2-PICALM. Transduced cells were subsequently induced for erythroid differentiation as described. The extent of erythroid differentiation was examined by FACS within GFP-positive (transduced) fractions. (I) Representative FACS profiles of WT- or PIP_2-PICALM-transduced cells after 3 days of culture. FACS profiles for GFP-positive fractions are shown. WT-PICALM fully rescued *Picalm* deficiency in erythroid development: greater than 40% of GFP-positive (WT-PICALM-transduced) cells were mature erythroblasts on day 3, while PIP_2-PICALM (or PH-PICALM)-transduced cells were not rescued. (J) Histograms show proportions of mature erythroblasts (%R4 and $\%FSC^{low}$ SSC^{low}) in empty vector-, PIP_2- or WT-PICALM-transduced cells after 3 days of culture. Experiments were repeated three times, and representative results are presented. Histograms: average value of two samples per condition; error bars: standard deviation.

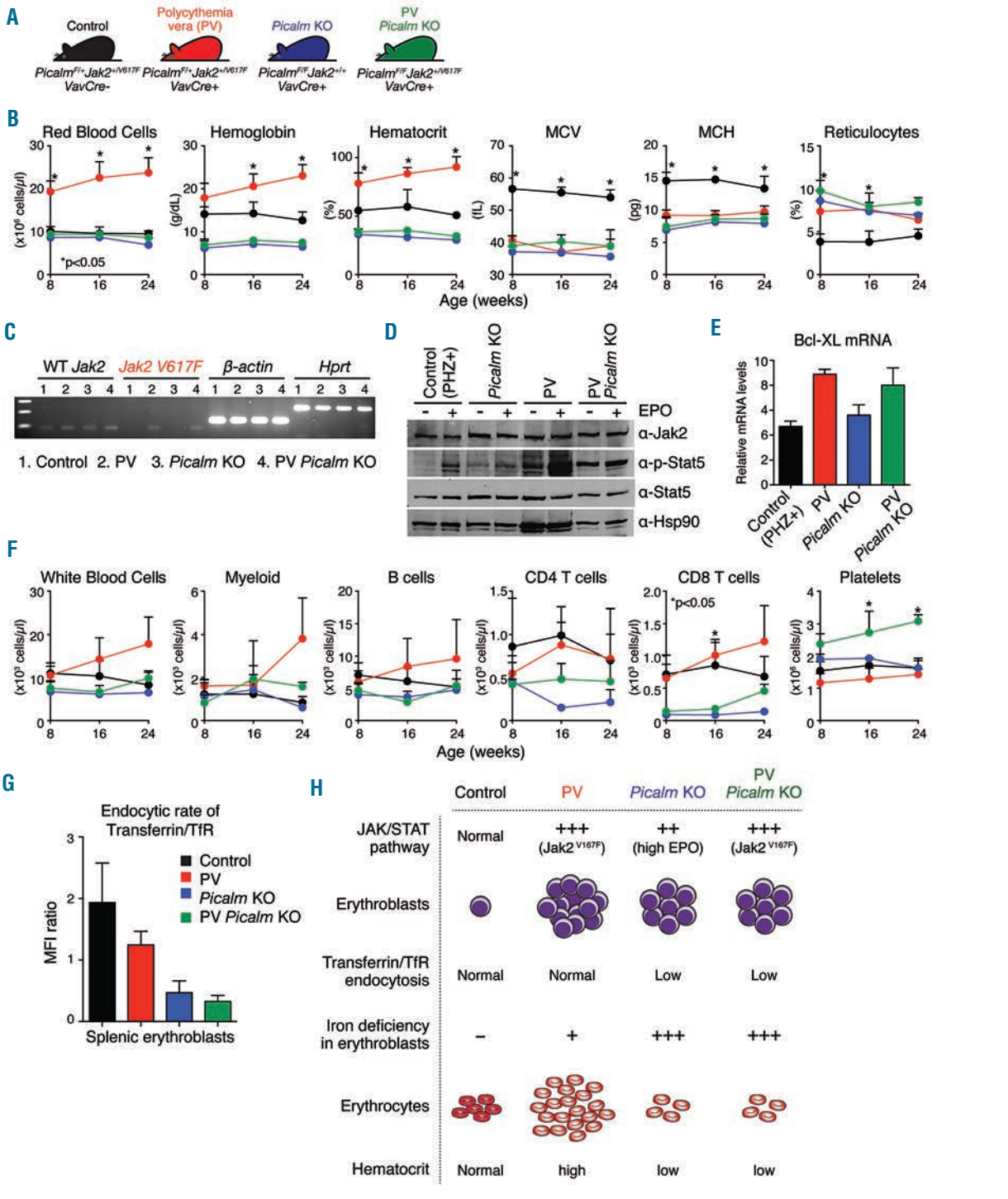

Figure 7. *Picalm* deletion ameliorates PV pathophysiology in mice. (A) Hematopoietic-specific *Picalm* conditional knockout mice were bred with PV mice (*Jak2*$^{+/V617F}$*Vav-Cre*$^{+}$) to generate *Picalm*-deficient PV mice (*Picalm*$^{F/F}$*Jak2*$^{+/V617F}$*Vav-Cre*$^{+}$). Four indicated groups were analyzed. (B) Time-course analysis of peripheral blood. *Picalm*-deficient PV mice (green line) exhibited a marked reduction in red blood cell counts, hemoglobin and hematocrit compared to PV mice (red line). Graphs represent average values of three of eight mice for each genotype. Error bars: standard deviation. (C) Total RNA was extracted from PB without red blood cell lysis and cDNA was prepared using standard methodology. Expression of WT and mutant *Jak2* (*Jak2* ^{V617F}) mRNA was analyzed by reverse transcription polymerase chain reaction (RT-PCR) using allele-specific primers as described.[27] Mutant *Jak2* transcripts were detected only in PB samples from PV and Picalm-deficient PV mice. RT-PCR for the housekeeping genes *β-actin* and *Hprt* was also performed. A representative gel is shown. (D) Jak2 kinase activity was examined by western blotting for the phosphorylated form of Stat5 (p-Stat5). Splenic erythroblasts were serum-starved for 2 h, treated with erythropoietin (EPO) for 10 min and protein extracts prepared. Western blot for Jak2 and Stat5 are also shown. Hsp90: loading control. Splenic erythroblasts of control mice were obtained after phenylhydrazine (PHZ) treatment. (E) mRNA levels of Bcl-XL in splenic erythroblasts were examined by realtime quantitative RT-PCR. (F) Time-course analysis of myeloid and lymphoid cell counts in PB. (G) Endocytic rate of transferrin/TfR in splenic erythroblasts was measured by FACS as described. (H) The *Jak2* ^{V617F} mutation causes constitutive activation of the Jak/Stat pathway in erythroid progenitors, leading to expansion of immature erythroblasts. PV mice exhibit a relative iron deficiency due to erythroid cell overproduction. In *Picalm* knockout (KO) mice, serum erythropoietin (EPO) levels are high and EPO/EPOR-mediated Jak/Stat signals are activated in erythroblasts; however, erythropoiesis (mature red cell production) is inefficient as TfR-mediated cellular iron uptake is impaired. In *Picalm*-deficient PV mice, regardless of *Jak2* ^{V617F}-driven Jak2/Stat5 activation, *Picalm* deficiency limits iron availability in erythroblasts, blocking red cell overproduction.

(*Jak2*$^{+/V617F}$ *Vav-Cre*$^{+}$).[26,27] Hematopoietic-specific *Picalm* knockout mice (*Picalm*$^{F/F}$ *Vav-Cre*$^{+}$) are viable and phenocopy *Picalm*$^{F/F}$ *Mx1Cre*$^{+}$ mice. We established and analyzed four groups of mice (Figure 7A). Mice with PV had significantly increased red blood cell counts and hemoglobin levels as well as elevated hematocrit,[26] while *Picalm*$^{F/F}$ *Vav-Cre*$^{+}$ mice exhibited microcytic anemia (Figure 7B). Despite expression of mutant Jak2 (Figure 7C), *Picalm*-deficient PV mice (PV *Picalm* knockout) developed microcytic and hypochromic anemia, as did *Picalm* knockout mice (Figure 7B). Importantly, *Picalm* deficiency did not alter Jak2 kinase activity (Figure 7D) and mRNA levels of Bcl-XL, a Jak/Stat target, were unaffected (Figure 7E). Although statistically insignificant, white blood cell counts, specifically counts of Gr-1^{+}CD11b^{+} myeloid cells, appeared low in *Picalm*-deficient PV mice. T-cell numbers were reduced in *Picalm* knockout and *Picalm*-deficient PV mice, as observed in *Picalm*$^{F/F}$ *Mx1-Cre*$^{+}$ mice (Figure 7F). Mild thrombocytosis, which was likely due to secondary effects of severe iron-deficiency,[28] was observed in *Picalm*-deficient PV mice (Figure 7F). As expected, TfR endocytosis was impeded in erythroblasts of *Picalm* knockout and *Picalm*-deficient PV mice (Figure 7G). Taken together, *Picalm* deficiency limits iron uptake in PV erythroblasts, effectively abrogating the polycythemia phenotype seen in these animals.

Discussion

PICALM binds to PIP_2 in the plasma membrane through its N-terminal ANTH domain and interacts with clathrin and other accessory proteins to form clathrin cargo, presumably playing a key role in clathrin-coated pit formation.[5-7] PICALM loss reportedly decreases uptake of specific r-SNARE associated with endosomal traffic.[22] This effect has been noted in cells maintained in culture; of note, most tissues in mice lacking Picalm appear normal, suggesting either a very restricted role of Picalm in the intracellular traffic of these r-SNARE or the up-regulation of a compensatory route. Knockout of *AP180*, a *PICALM* homolog, in flies results in slightly larger synaptic vesicles than those seen in normal flies;[29,30] however, *PICALM* depletion by short interfering RNA in cell lines has no effect on receptor-mediated transferrin uptake and a minimal effect on the morphology of clathrin coats.[7,31-33] Our visualization studies with MEF indicate relatively modest effects on endocytic coat dynamics attained upon simultaneous depletion of both Ap180 and Picalm whereas no detectable effects were observed in MEF subjected to Ap180 or Picalm depletion alone. The increase in lifetime combined with the decrease in the number of mature coated pits/vesicles are effects that can account for the observed decrease of transferrin uptake in erythroblasts.

It has been shown that anemia-promoting mutations at the *Fit1* locus in mice occur in the *Picalm* gene.[34-36] Studies of *Fit1* mutants, although useful, do not represent an ideal model for understanding the role of PICALM, because they are heterozygous for a *Picalm* point mutation and harbor the *Del*^{26DVT} deletion in the other allele, removing a 11cM segment including the *Picalm* gene.[34-36] Suzuki and colleagues recently reported a conventional *Picalm* knockout strain.[37] They reported that more than 90% of *Picalm*$^{-/-}$ newborn pups die before weaning and body weights of surviving *Picalm*$^{-/-}$ mice are significantly lower than those of controls.[37] Since the surviving *Picalm*$^{-/-}$ mice had severe growth retardation and liver damage, it is likely that the hematopoietic phenotypes of these mice are secondary effects of the growth retardation and liver dysfunction. In fact, these phenotypes differ significantly from those of conditional knockout models. Although severe B-cell defects have been reported in *Picalm*$^{-/-}$ mice, none of our conditional or transplant models exhibited a B-cell phenotype. While we observed significant expansion of immature erythroblasts exhibiting inefficient erythropoiesis (Figures 2 and 3), Suzuki *et al.* observed somewhat reduced numbers of erythroblasts in the bone marrow and spleen.[37]

Phenotypes observed in *Picalm* knockout mice differ from those seen in clinically prevalent iron-deficiency anemia (e.g. the former have high reticulocyte counts and high serum iron levels). In contrast to the situation in typical iron-deficiency anemia, iron is not "absolutely deficient" in *Picalm* knockout mice. Transferrin-bound iron is abundant in the sera of *Picalm* knockout mice (Figure 1), and levels of transferrin-bound surface TfR increase in *Picalm*-deficient erythroblasts (Figure 4). Thus, *Picalm*-deficient erythroblasts may take up transferrin-bound iron through a "clathrin-independent" endocytosis pathway (e.g. fluid-phase uptake).[38] Such a pathway may provide *Picalm*-deficient erythroblasts with the minimum amount of iron required to give rise to reticulocytes under strong erythropoietic conditions. Alternatively, since the transition from reticulocytes to erythrocytes is accompanied by extensive structural changes in the plasma membrane and elimination of organelles,[39,40] Picalm deficiency may impair reticulocyte maturation by modulating these pathways.

TfR-deficient (*TfR*$^{-/-}$) embryonic stem cells give rise to bone marrow B cells in chimeric mice; however, T-cell development is arrested at the CD4/8 DN stage, suggesting that TfR is indispensable for immature T-cell development in the thymus.[14] We found that T-cell development in the thymus of *Picalm*$^{F/F}$ *Mx1Cre*$^{+}$ mice was grossly normal, and the numbers of CD4^{-} and CD8^{-} T cells in peripheral blood were reduced to the same extent (Figure 2B). These data suggest that the observed T-cell phenotype is not due to a block of differentiation at a specific stage of T-cell development. It is possible that a small fraction of CD4/8 DN T cells require Picalm-mediated TfR endocytosis, causing a mild T-lymphopenia in *Picalm*$^{F/F}$ *Mx1Cre*$^{+}$ mice.

Erythroid progenitors give rise to red blood cells in culture without the support of other lineage cells.[11] *In vivo*, however, erythroid progenitors differentiate into red blood cells in a specialized niche called the erythroblastic island.[41] Several cell adhesion molecules and their interacting partners within erythroblastic islands are reportedly necessary for island integrity.[42,43] Central macrophages supposedly provide nutrients and growth factors, including iron, to erythroblasts and function to induce erythroid maturation.[41,44,45] *TfR* knockout mice die *in utero* due to anemia before embryonic day 12.5; however, *TfR*-deficient embryos can produce a substantial amount of red cell mass as late as 10.5 d.p.c.[46] In contrast, yolk sac-derived *TfR*-deficient progenitors do not give rise to erythroid colonies *in vitro*,[46] suggesting that the "TfR-independent" iron uptake pathway is available only *in vivo*. We see similar phenotypes in *Picalm* conditional knockout mice: *Picalm*-deficient hematopoietic progenitors do not give rise to erythroblasts *in vitro*, while erythroblasts are greatly expanded in spleen and bone marrow. There are a few explanations for the observed discrepancies between *in*

vivo and *in vitro* phenotypes. *Picalm*-deficient erythroid progenitors could take up transferrin-bound iron through a Picalm-independent pathway *in vivo* (for example via direct contact with surrounding cells). Alternatively, non-transferrin-bound iron, potentially available in the local micro-environment, could supply a minimal amount of iron for erythroblast survival *in vivo*.

Iron chelators are widely used in the clinic to prevent organ damage due to iron overload.[47] At the therapeutic dosage, they target primarily non-transferrin-bound iron, while transferrin-bound iron remains intact.[48] Since highly proliferating cells depend on metalloenzymes, iron and its internalization pathways are considered attractive targets for cancer therapy. Iron chelators have been tested for anti-tumor activity[49] and, as hematologic cancer cells generally express high surface levels of TfR, multiple TfR antibodies have been tested as anti-cancer agents over the last 25 years.[50] Our findings suggest a novel strategy to target transferrin-bound iron. *Picalm* deletion causes iron deficiency in PV erythroblasts leading to reduced red cell mass, and completely abrogates the polycythemia disease phenotype in mice (Figure 7B). Since global *Picalm* inactivation did not cause gross defects in mouse fitness (*Online Supplementary Figure S6*), targeting PICALM for hematologic malignancies might be feasible and warrants attention as a therapeutic approach. Since PICALM is abundant in a series of cancer cells, our *Picalm* conditional strain may be useful to assess effects of *Picalm* deletion in mouse cancer models.

While clathrin-dependent endocytosis has been thought to employ a "common machinery" shared by all cell types, we propose a cell type-specific endocytic machinery regulated by PICALM in erythroblasts. Furthermore, our study identifies molecular mechanisms required for efficient iron uptake in erythroblasts.

Acknowledgments

We thank members of COH Animal Resources and ARCH for colony maintenance; Walter Tsark for help and advice on generation of Picalm knockout mice; Robyn Roth for help on freeze-etch electron microscopy. Jing Zhang, Jiahai Shi and Harvey Lodish for sharing experimental protocols; Taisuke Kondo, Julio Valencia, Vincent Hearing, Barry Paw, Carlo Brugnara, Paul Schmidt and Mark Fleming for advice; Thomas Ludwig for ROSA26$^{Cre\text{-}ERT2}$ mice; Jean Christophe Zeeh, Patrick Reeves, and Raphael Gaudin for technical advice; and Mai Suzuki and other members of the Maeda laboratory for help and advice. This work was supported in part by the National Institutes of Health (grant R01 GM075252 to TK), the Japan Society for the Promotion of Science (Young Researcher Overseas Visits Program for Vitalizing Brain Circulation fellowship to YI) and the American Cancer Society (grant RSG-13-379-01-LIB to TM).

Authorship and Disclosures

Information on authorship, contributions, and financial & other disclosures was provided by the authors and is available with the online version of this article at www.haematologica.org.

References

1. Jandl JH, Inman JK, Simmons RL, Allen DW. Transfer of iron from serum iron-binding protein to human reticulocytes. J Clin Invest. 1959;38(1, Part 1):161-185.
2. Harding C, Heuser J, Stahl P. Receptor-mediated endocytosis of transferrin and recycling of the transferrin receptor in rat reticulocytes. J Cell Biol. 1983;97(2):329-339.
3. Ciechanover A, Schwartz AL, Dautry-Varsat A, Lodish HF. Kinetics of internalization and recycling of transferrin and the transferrin receptor in a human hepatoma cell line. Effect of lysosomotropic agents. J Biol Chem. 1983;258(16):9681-9689.
4. Andrews NC. Forging a field: the golden age of iron biology. Blood. 2008;112(2):219-230.
5. Tebar F, Bohlander SK, Sorkin A. Clathrin assembly lymphoid myeloid leukemia (CALM) protein: localization in endocytic-coated pits, interactions with clathrin, and the impact of overexpression on clathrin-mediated traffic. Mol Biol Cell. 1999;10(8): 2687-2702.
6. Ford MG, Pearse BM, Higgins MK, et al. Simultaneous binding of PtdIns(4,5)P2 and clathrin by AP180 in the nucleation of clathrin lattices on membranes. Science. 2001;291(5506):1051-1055.
7. Meyerholz A, Hinrichsen L, Groos S, Esk PC, Brandes G, Ungewickell EJ. Effect of clathrin assembly lymphoid myeloid leukemia protein depletion on clathrin coat formation. Traffic. 2005;6(12):1225-1234.
8. Dreyling MH, Martinez-Climent JA, Zheng M, Mao J, Rowley JD, Bohlander SK. The t(10;11)(p13;q14) in the U937 cell line results in the fusion of the AF10 gene and CALM, encoding a new member of the AP-3 clathrin assembly protein family. Proc Natl Acad Sci USA. 1996;93(10):4804-4809.
9. Harold D, Abraham R, Hollingworth P, et al. Genome-wide association study identifies variants at CLU and PICALM associated with Alzheimer's disease. Nat Genet. 2009;41(10): 1088-1093.
10. Xu J, Shao Z, Glass K, et al. Combinatorial assembly of developmental stage-specific enhancers controls gene expression programs during human erythropoiesis. Dev Cell. 2012;23(4):796-811.
11. Zhang J, Socolovsky M, Gross AW, Lodish HF. Role of Ras signaling in erythroid differentiation of mouse fetal liver cells: functional analysis by a flow cytometry-based novel culture system. Blood. 2003;102(12):3938-3946.
12. Ji P, Jayapal SR, Lodish HF. Enucleation of cultured mouse fetal erythroblasts requires Rac GTPases and mDia2. Nat Cell Biol. 2008;10(3):314-321.
13. Kühn R, Schwenk F, Aguet M, Rajewsky K. Inducible gene targeting in mice. Science. 1995;269(5229):1427-1429.
14. Ned RM, Swat W, Andrews NC. Transferrin receptor 1 is differentially required in lymphocyte development. Blood. 2003;102(10): 3711-3718.
15. Socolovsky M, Nam H, Fleming MD, Haase VH, Brugnara C, Lodish HF. Ineffective erythropoiesis in Stat5a-/-5b-/-mice due to decreased survival of early erythroblasts. Blood. 2001;98(12):3261.
16. Chen K, Liu J, Heck S, Chasis JA, An X, Mohandas N. Resolving the distinct stages in erythroid differentiation based on dynamic changes in membrane protein expression during erythropoiesis. Proc Natl Acad Sci USA. 2009;106(41): 17413-17418.
17. Heuser J. Protocol for 3-D visualization of molecules on mica via the quick-freeze, deep-etch technique. J Electron Microsc Tech. 1989;13(3):244-263.
18. Kirchhausen T. Imaging endocytic clathrin structures in living cells. Trends Cell Biol. 2009;19(11):596-605.
19. Ehrlich M, Boll W, Van Oijen A, et al. Endocytosis by random initiation and stabilization of clathrin-coated pits. Cell. 2004;118(5):591-605.
20. Cocucci E, Aguet F, Boulant S, Kirchhausen T. The first five seconds in the life of a clathrin-coated pit. Cell. 2012;150(3):495-507.
21. Aguet F, Antonescu CN, Mettlen M, Schmid SL, Danuser G. Advances in analysis of low signal-to-noise images link dynamin and AP2 to the functions of an endocytic checkpoint. Dev Cell. 2013;26(3):279-291.
22. Miller SE, Sahlender DA, Graham SC, et al. The molecular basis for the endocytosis of small R-SNAREs by the clathrin adaptor CALM. Cell. 2011;147(5):1118-1131.
23. Shuga J, Zhang J, Samson LD, Lodish HF, Griffith LG. In vitro erythropoiesis from bone marrow-derived progenitors provides a physiological assay for toxic and mutagenic compounds. Proc Natl Acad Sci USA. 2007;104(21):8737-8742.
24. Kaplan J, Jordan I, Sturrock A. Regulation of the transferrin-independent iron transport system in cultured cells. J Biol Chem. 1991;266(5):2997-3004.
25. Cheng HF, Jiang MJ, Chen CL, et al. Cloning and identification of amino acid residues of human phospholipase C delta 1 essential for catalysis. J Biol Chem. 1995;270(10):5495-5505.
26. Mullally A, Lane SW, Ball B, et al. Physiological Jak2V617F expression causes a lethal myeloproliferative neoplasm with dif-

ferential effects on hematopoietic stem and progenitor cells. Cancer Cell. 2010;17(6): 584-596.
27. Mullally A, Lane SW, Brumme K, Ebert BL. Myeloproliferative neoplasm animal models. Hematol Oncol Clin North Am. 2012;26(5):1065-1081.
28. Franchini M, Targher G, Montagnana M, Lippi G. Iron and thrombosis. Ann Hematol. 2008;87(3):167-173.
29. Ahle S, Ungewickell E. Purification and properties of a new clathrin assembly protein. EMBO J. 1986;5(12):3143-3149.
30. Zhang B, Koh YH, Beckstead RB, Budnik V, Ganetzky B, Bellen HJ. Synaptic vesicle size and number are regulated by a clathrin adaptor protein required for endocytosis. Neuron. 1998;21(6):1465-1475.
31. Huang F, Khvorova A, Marshall W, Sorkin A. Analysis of clathrin-mediated endocytosis of epidermal growth factor receptor by RNA interference. J Biol Chem. 2004;279(16): 16657-16661.
32. Harel A, Wu F, Mattson MP, Morris CM, Yao PJ. Evidence for CALM in directing VAMP2 trafficking. Traffic. 2008;9(3):417-429.
33. Kozik P, Hodson NA, Sahlender DA, et al. A human genome-wide screen for regulators of clathrin-coated vesicle formation reveals an unexpected role for the V-ATPase. Nat Cell Biol. 2013;15(1): 50-60.
34. Potter MD, Klebig ML, Carpenter DA, Rinchik EM. Genetic and physical mapping of the fitness 1 (fit1) locus within the Fes-Hbb region of mouse chromosome 7. Mamm Genome. 1995;6(2):70-75.
35. Potter MD, Shinpock SG, Popp RA, et al. Mutations in the murine fitness 1 gene result in defective hematopoiesis. Blood. 1997;90(5):1850-1857.
36. Klebig ML, Wall MD, Potter MD, Rowe EL, Carpenter DA, Rinchik EM. Mutations in the clathrin-assembly gene Picalm are responsible for the hematopoietic and iron metabolism abnormalities in fit1 mice. Proc Natl Acad Sci USA. 2003;100(14):8360-8365.
37. Suzuki M, Tanaka H, Tanimura A, et al. The clathrin assembly protein PICALM is required for erythroid maturation and transferrin internalization in mice. PLoS One. 2012;7(2):e31854.
38. Sandvig K, Pust S, Skotland T, van Deurs B. Clathrin-independent endocytosis: mechanisms and function. Curr Opin Cell Biol. 2011;23(4):413-420.
39. Liu J, Guo X, Mohandas N, Chasis JA, An X. Membrane remodeling during reticulocyte maturation. Blood. 2010;115(10): 2021-2027.
40. Ashrafi G, Schwarz TL. The pathways of mitophagy for quality control and clearance of mitochondria. Cell Death Differ. 2013;20 (1):31-42.
41. Manwani D, Bieker JJ. The erythroblastic island. Curr Top Dev Biol. 2008;82:23-53.
42. Hanspal M, Smockova Y, Uong Q. Molecular identification and functional characterization of a novel protein that mediates the attachment of erythroblasts to macrophages. Blood. 1998;92(8):2940-2950.
43. Lee G, Lo A, Short SA, et al. Targeted gene deletion demonstrates that the cell adhesion molecule ICAM-4 is critical for erythroblastic island formation. Blood. 2006;108(6): 2064-2071.
44. Ramos P, Casu C, Gardenghi S, et al. Macrophages support pathological erythropoiesis in polycythemia vera and β-thalassemia. Nat Med. 2013;19(4):437-445.
45. Chow A, Huggins M, Ahmed J, et al. CD169^{+} macrophages provide a niche promoting erythropoiesis under homeostasis and stress. Nat Med. 2013;19(4):429-436.
46. Levy JE, Jin O, Fujiwara Y, Kuo F, Andrews NC. Transferrin receptor is necessary for development of erythrocytes and the nervous system. Nat Genet. 1999;21(4): 396-399.
47. Hoffbrand AV, Taher A, Cappellini MD. How I treat transfusional iron overload. Blood. 2012;120(18):3657-3669.
48. Evans RW, Kong X, Hider RC. Iron mobilization from transferrin by therapeutic iron chelating agents. Biochim Biophys Acta. 2012;1820(3):282-290.
49. Merlot AM, Kalinowski DS, Richardson DR. Novel chelators for cancer treatment: where are we now? Antioxid Redox Signal. 2013;18(8):973-1006.
50. Daniels TR, Delgado T, Rodriguez JA, Helguera G, Penichet ML. The transferrin receptor part I: Biology and targeting with cytotoxic antibodies for the treatment of cancer. Clin Immunol. 2006;121(2):144-158.
51. Maeda T, Merghoub T, Hobbs RM, et al. Regulation of B versus T lymphoid lineage fate decision by the proto-oncogene LRF. Science. 2007;316(5826):860-866.
52. Pronk CJ, Rossi DJ, Månsson R, et al. Elucidation of the phenotypic, functional, and molecular topography of a myeloerythroid progenitor cell hierarchy. Cell Stem Cell. 2007;1(4):428-442.